

# Bayesian selection of misspecified models is overconfident and may cause spurious posterior probabilities for phylogenetic trees

Ziheng Yang<sup>\*, †</sup> and Tianqi Zhu<sup>‡</sup>

<sup>\*</sup>Department of Genetics, University College London, Gower Street, London WC1E 6BT, UK, <sup>†</sup>Radcliffe Institute for Advanced Studies, Harvard University, Cambridge, MA 02138, USA, and <sup>‡</sup>Institute of Applied Mathematics, Academy of Mathematics and Systems Science, Chinese Academy of Sciences, Beijing 100190, China

Submitted to Proceedings of the National Academy of Sciences of the United States of America

The Bayesian method is noted to produce spuriously high posterior probabilities for phylogenetic trees in analysis of large datasets, but the precise reasons for this over-confidence are unknown. In general, the performance of Bayesian selection of misspecified models is poorly understood, even though this is of great scientific interest since models are never true in real data analysis. Here we characterize the asymptotic behavior of Bayesian model selection and show that when the competing models are equally wrong, Bayesian model selection exhibits surprising and polarized behaviors in large datasets, supporting one model with full force while rejecting the others. If one model is slightly less wrong than the other, the less wrong model will eventually win when the amount of data increases, but the method may become overconfident before it becomes reliable. We suggest that this extreme behavior may be a major factor for the spuriously high posterior probabilities for evolutionary trees observed in molecular phylogenetics. The philosophical implications of our results to the application of Bayesian model selection to evaluate opposing scientific hypotheses are yet to be explored, as are the behaviors of non-Bayesian methods in similar situations.

Bayesian inference | fair-coin paradox | model selection | posterior probability  
| star-tree paradox

## Introduction

The Bayesian method was introduced into molecular phylogenetics in the 1990s [1, 2, 3] and has since become one of the most popular methods for statistical analysis in the field, in particular, for estimation of species phylogenies [4, 5, 6, 7]. It has been noted that the method often produces very high posterior probabilities for trees or clades (nodes in the tree). In the first ever Bayesian phylogenetic calculation, a biologically reasonable tree for five species of great apes was produced from a dataset of 11 mitochondrial tRNA genes (739 sites), but the posterior probability for that tree, at 0.9999, was uncomfortably high [1]. In the past two decades, the Bayesian method has been used to analyze thousands of datasets, with the computation made possible through Markov chain Monte Carlo (MCMC) [4, 5]. It has become a common practice to report posterior clade probabilities only if they are  $< 100\%$  (because most estimates are 100%). In some cases the high posterior probabilities are decidedly spurious. For example, conflicting trees may be inferred from the same data under different evolutionary models, each with strong support. Different trees may be inferred depending on the species sampled in the dataset [8], or on whether protein sequences or the encoding DNA sequences are analyzed [9]. In such cases, the different trees cannot all be correct, even if the true tree is unknown. The concern is not so much that the inferred species relationships may be wrong as that they are supported by extremely high posterior probabilities.

In the *star-tree paradox*, large datasets were simulated using the star tree, and then analyzed to calculate the posterior probabilities for the three binary trees (Fig. 1). Most biologists would like the posterior probabilities for the binary trees to converge to  $(\frac{1}{3}, \frac{1}{3}, \frac{1}{3})$  when the amount of data increases [10, 11, 12]. Instead they fluctuate among datasets according to a statistical distribution, sometimes producing

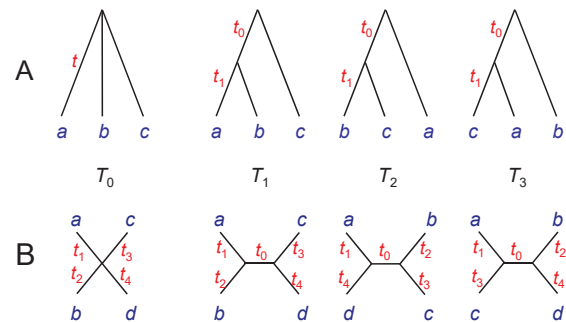


**Fig. 1.** (A) The three binary rooted trees for three species  $T_1, T_2$ , and  $T_3$  and the star tree  $T_0$ . (B) The three binary unrooted trees for four species  $T_1, T_2$ , and  $T_3$  and the star tree  $T_0$ . The branch length parameters are shown next to the branches, measured by the expected number of nucleotide changes per site. In the star-tree simulations, the star tree is used to generate data, which are analyzed to calculate the posterior probabilities for the three binary trees, with the star tree excluded.

strong support for a binary tree even though the data do not contain any information either for or against any binary tree [13, 14, 15].

Bayesian model selection is known to be consistent [16]. When the data size  $n \rightarrow \infty$ , the true model ‘dominates’, with its posterior probability approaching 1. If several models are equally right, the model with fewer parameters dominates. However, this theory applies only if the true model is included in the comparison. Given that a model is a simplified representation of the physical world, the more common

## Significance

The Bayesian method is widely used to estimate species phylogenies using molecular sequence data. While it has long been noted to produce spuriously high posterior probabilities for trees or clades, the precise reasons for this overconfidence are unknown. Here we characterize the behavior of Bayesian model selection when the compared models are misspecified, and demonstrate that when the models are nearly equally wrong, the method exhibits unpleasant polarized behaviors, supporting one model with high confidence while rejecting others. This provides an explanation for the empirical observation of spuriously high posterior probabilities in molecular phylogenetics.

## Reserved for Publication Footnotes

situation in real data analysis should be the comparison of models that are all wrong. Not many theoretical results appear to exist concerning Bayesian comparison of misspecified models [17].

Here we study the asymptotic behavior of Bayesian model selection in a general setting where multiple misspecified models are compared. We are interested in how the posterior probabilities for models behave when the data size increases. Does the dynamics depend on whether there are any free parameters in the models? If one model is less wrong than another (in a certain sense appropriately defined), will the less wrong model always win? We present the proofs and mathematical analyses in SI Appendix. In the main paper, we summarize our results and illustrate them using three canonical simple problems. Our analysis suggests that the problem exposed by the star tree-paradox is actually far more troubling than discussed previously [11, 12, 13, 14, 15].

## Results

**Problem description.** We consider independent and identically distributed (i.i.d.) models only. The data  $x = \{x_1, \dots, x_n\}$  are an i.i.d. sample from the true model  $g(\cdot)$ . We consider two models as the case for more models is obvious. Model  $H_k$  has density  $f_k(x|\theta_k)$ , with  $d_k$  free parameters ( $\theta_k$ ),  $k = 1, 2$ . We are in particular interested in models of the same dimension, with  $d_1 = d_2 = d$ . In the Bayesian analysis, we assign a uniform prior for the two models ( $\pi_1 = \pi_2 = \frac{1}{2}$ ) and also a prior for the parameters within each model  $H_k$ :  $f_k(\theta_k)$ . The posterior model probabilities,  $P_k = \mathbb{P}(H_k|x)$ , are then proportional to the marginal likelihoods:  $M_k = f_k(x) = \int f_k(\theta_k)f_k(x|\theta_k)d\theta_k$ ; that is,  $P_1/P_2 = (\pi_1 M_1)/(\pi_2 M_2) = M_1/M_2$ . We are interested in the asymptotic behavior of  $P_1$  in large datasets (as  $n \rightarrow \infty$ ).

The dynamics depends on how well the models fit the data. Let  $\hat{\theta}_k$  be the maximum likelihood estimate (MLE) of  $\theta_k$  under model  $H_k$  from dataset  $x$ . Let  $\theta_k^*$  be the limiting value of  $\hat{\theta}_k$  when the data size  $n \rightarrow \infty$ . In other words  $\theta_k^*$  minimizes the Kullback-Leibler (K-L) divergence from model  $H_k$  to the true model

$$D_k = D_{\text{KL}}(g, f_k) = \int g(x) \log g(x) dx - \int g(x) \log f_k(x|\theta_k^*) dx, \quad [1]$$

and is known as the *best-fitting* or *pseudo-true* parameter value under the model [18].  $D_k$  (calculated at  $\theta_k^*$ ) measures the distance from  $H_k$  to the true model, with  $D_k \geq 0$ . We say a model is ‘right’ if it encompasses the true model, with  $D = 0$ , and ‘wrong’ if  $D > 0$ . Model 1 is less wrong than model 2 if  $D_1 < D_2$ . Both models are ‘equally right’ if  $D_1 = D_2 = 0$  and ‘equally wrong’ if  $D_1 = D_2 > 0$ .

**Characterization of Bayesian model selection.** The asymptotic behavior of  $P_1 = \mathbb{P}(H_1|x)$  when  $n \rightarrow \infty$  is analyzed in SI Appendix and summarized in Fig. 2. We identify three types of asymptotic behaviors: type-1 (‘balanced’), type-2 (‘volatile’) and type-3 (‘polarized’), as defined below. We also refer to three types of inference problems that give rise to those behaviors.

Type 1 (‘balanced’) is for the posterior model probability  $P_1$  to converge (as  $n \rightarrow \infty$ ) to a single reasonable value that is different from 0 and 1, such as  $\frac{1}{2}$ . In other words, in essentially every large dataset,  $P_1 \approx \frac{1}{2}$ . This behavior occurs when the two models are essentially identical. Examples include comparison of two identical models with no parameters, such as  $H_1 : p = 0.5$  and  $H_2 : p = 0.5$  irrespective of the true  $p$  in a coin-tossing experiment (Fig. 2 cases  $A_1$  and  $A_2$ ), and overlapping models where the best-fitting parameter values lie in the region of overlap (Fig. 2,  $A_3$  and  $A_4$ ). Whether the two models are both right ( $A_1$  and  $A_3$ ) or both wrong ( $A_2$  and  $A_4$ ) does not affect the dynamics. The case of overlapping models is interesting. If the truth is  $p = \frac{1}{2}$  while the two compared models are  $H_1 : 0.4 < p < 0.6$  and  $H_2 : 0 < p < 1$ , and if we assign a uniform prior on  $p$  in each model, then as  $n \rightarrow \infty$ ,  $P_1 \rightarrow \frac{1}{1+0.2} = \frac{5}{6}$ , which appears more rea-

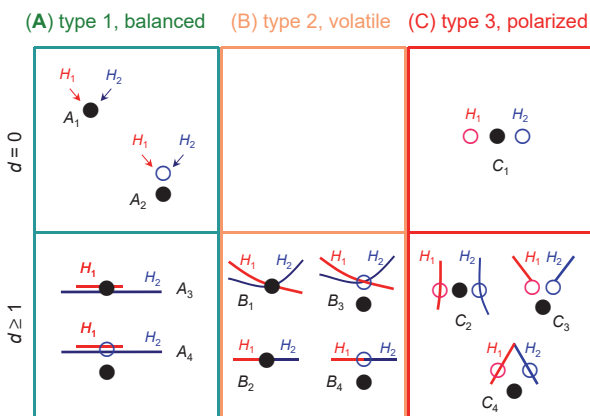


**Fig. 2.** Classification of Bayesian model-selection problems involving two equally right or equally wrong models, each with  $d$  free parameters. Solid circles represent the true model, while the lines represent the parameter space of the compared models, with the empty circles to be the best-fitting parameter value ( $\theta^*$ ). The two models are equally right (with  $D_1 = D_2 = 0$ ) if the solid and empty circles coincide, and equally wrong (with  $D_1 = D_2 > 0$ ) if they are separate. The models are ‘indistinct’ if the two empty circles coincide (as in A and B), and are ‘distinct’ if they are separate (as in C). The boxes indicate the three different asymptotic behaviors of Bayesian model selection when the data size  $n \rightarrow \infty$ : A: ‘balanced’ (green) for identical or overlapping models; B: ‘volatile’ (orange) for indistinct models; and C: ‘polarized’ (red) for distinct models.

sonable than  $\frac{1}{2}$  as it favors the more-informative model  $H_1$ . At any rate, the comparison of identical or overlapping models is unusual for testing scientific hypotheses. This type of problem is not considered further.

Type 2 (‘volatile’) is for  $P_1$  to converge to a nondegenerate statistical distribution, such as  $U(0, 1)$ . In other words, if we analyze different large datasets, all generated from the same true model, to compare two equally right or equally wrong models,  $P_1$  varies among datasets according to a nondegenerate distribution. This behavior occurs when the two compared models become unidentifiable as the data size  $n \rightarrow \infty$ . There are two scenarios. In the first, both models are right, with  $D_1 = D_2 = 0$  (Fig. 2,  $B_1$  and  $B_2$ ). In the second both models are equally wrong (with  $D_1 = D_2 > 0$ ) but indistinct (Fig. 2,  $B_3$  and  $B_4$ ). We say that two models are indistinct if and only if they, each at the best-fitting parameter values, are unidentifiable, with  $f_1(x|\theta_1^*) = f_2(x|\theta_2^*)$  for essentially all  $x$ . In other words, in infinite data, the two models make essentially the same predictions about the data and are unidentifiable. In both scenarios of equally right and equally wrong models,  $P_1$  varies among datasets according to a non-degenerate distribution.

Type 3 (‘polarized’) is for  $P_1$  to have a degenerate two-point distribution, at values 0 and 1. If we analyze large datasets to compare two models, we favour model 1 with total confidence in some datasets and model 2 with total confidence in others. This behavior is observed when the two models are equally wrong and also distinct.

It is remarkable that the asymptotic behavior is determined by whether or not the compared models are distinct, and not by whether they are both right or both wrong, or by whether the compared models have unknown parameters. For example, cases  $B_1$  (two right models) and  $B_3$  (two equally wrong models) in Fig. 2 show the same ‘volatile’ behavior, while cases  $C_1$  (no free parameters) and  $C_2$  (with free parameters) show the same ‘polarized’ behavior.

**Problem 1. Fair-coin paradox (equally wrong models with no free parameter).** Consider a coin-tossing experiment in which the coin is fair with the probability of heads  $p = \frac{1}{2}$ . We use the data of  $x$  heads in  $n$  tosses to compare two models:  $H_1 : p = 0.4$  (tail bias) and  $H_2 : p = 0.6$  (head bias). The two models are equally wrong. We assign a uniform prior for the two models ( $\frac{1}{2}$  each), and calculate the

posterior model probability  $P_1 = \mathbb{P}(H_1|x)$ . This is a type-3 problem (Fig. 2,  $C_1$ ).

As the models involve no free parameters, the likelihood ( $L$ ) and marginal likelihood ( $M$ ) are the same, given by the binomial probability for data  $x$ . The posterior odds is the likelihood ratio

$$\frac{P_1}{1-P_1} = \frac{M_1}{M_2} = \frac{0.4^x \cdot 0.6^{n-x}}{0.6^x \cdot 0.4^{n-x}} = \left(\frac{0.4}{0.6}\right)^{2x-n}. \quad [2]$$

When  $n$  is large,  $P_1$  tends to be extreme (close to 0 or 1). Indeed  $\alpha < P_1 < 1 - \alpha$  if and only if  $|2x - n| < B = \frac{\log\{\alpha/(1-\alpha)\}}{\log\{0.4/0.6\}}$ . If  $n$  is large,  $2x - n$  is approximately  $\mathbb{N}(0, n)$ , so that

$$\mathbb{P}\{|2x - n| < B\} \approx 1 - 2\Phi\left(-\frac{B}{\sqrt{n}}\right) \approx \frac{2B}{\sqrt{2\pi n}}, \quad [3]$$

where  $\Phi$  is the cumulative distribution function (CDF) for  $\mathbb{N}(0, 1)$ . If  $\alpha = 1\%$ , we have  $B = 11.33296$ , so that only 11 data outcomes will give  $P_1$  in the range  $(0.01, 0.99)$ , with  $x - \frac{n}{2}$  to be  $-5, -4, \dots, 5$ . For  $n = 10^3, 10^4, 10^5, 10^6$ , we have  $\mathbb{P}\{0.01 < P_1 < 0.99\} = 0.280, 0.090, 0.0286$ , and  $0.0090$  using the normal approximation of eq. [3], or  $0.272, 0.0876, 0.0277$ , and  $0.0088$  exactly by the binomial distribution. Thus in large datasets, moderate posterior probabilities will be rare, and either  $H_1$  or  $H_2$  will be favored with posterior  $> 0.99$ . When  $n \rightarrow \infty$ ,  $P_1$  has a degenerate two-point distribution, taking the values 0 and 1, each half of the times. This is the type-3 ‘polarized’ behavior. Note that there is no information either for or against either model in the data. Fig. 3A(i) shows the distribution of  $P_1$  for  $n = 10^3$ .

Fig. 3A(ii) shows the comparison of  $H_1 : p = 0.42$  against  $H_2 : p = 0.6$  when the truth is  $p = 0.5$ . Here  $H_1$  is less wrong and will eventually dominate. However, in large and finite datasets, the more wrong model  $H_2$  can often receive high support. For example, for  $n = 10^3$ , non-extreme posterior probabilities in the range  $0.01 < P_1 < 0.99$  occur for only 13 data outcomes, with  $x$  to be 504-516, and in 14.8% of datasets,  $x$  is greater than those values so that  $P_2 > 0.99$ . Indeed over the whole range  $36 \leq n \leq 11611$ , the more wrong model  $H_2$  is strongly favored too often, with  $\mathbb{P}(P_2 > 0.99) > 0.01$ . *The method becomes overconfident before it becomes reliable.* It may be noted that such strong support for the more wrong model occurs only when the two models are opposing each other. It does not occur if both models are wrong in the same direction: in the comparison of  $H_1 : p = 0.4$  and  $H_2 : p = 0.42$  when the truth is  $p = 0.5$ , the less wrong model  $H_2$  dominates in the posterior.

**Problem 2. Fair-balance paradox (equally right models or equally wrong and indistinct models).** The true model is  $\mathbb{N}(0, 1)$ , and we compare two models  $H_1 : \mathbb{N}(\mu, 1/\tau)$ ,  $\mu < 0$  and  $H_2 : \mathbb{N}(\mu, 1/\tau)$ ,  $\mu > 0$ , with  $\tau$  given. The data may represent measurement errors observed on a fair balance while the models claim that the balance has an unknown negative or positive bias. The best-fitting parameter value (the MLE when the data size  $n \rightarrow \infty$ ) is  $\mu^* = 0$  in each model, when the two models become identical (indistinct). Thus the two models are equally right if  $\tau = 1$  (Fig. 2,  $B_2$ ), and are equally wrong if  $\tau = 1/9$  or  $9$  (Fig. 2,  $B_4$ ).

We assign a uniform prior on the two models ( $\frac{1}{2}$  each), and  $\mu \sim \mathbb{N}(0, 1/\xi)$  with  $\xi$  fixed, truncated to the appropriate range under each model. The data ( $x$ ), an i.i.d. sample from  $\mathbb{N}(0, 1)$ , can be summarized as the sample mean  $\bar{x}$ . It can be shown that the posterior model probability  $P_1 = \mathbb{P}\{H_1|x\}$  varies among datasets according to the following density

$$f(P_1) = \frac{\sqrt{\tau + \xi/n}}{\tau} \cdot \exp\left\{\frac{[\Phi^{-1}(P_1)]^2}{2} \left[1 - \frac{1}{\tau} - \frac{\xi}{n\tau^2}\right]\right\}, \quad [4]$$

where  $\Phi^{-1}$  is the inverse CDF for  $\mathbb{N}(0, 1)$  (SI Appendix).

Fig. 3B shows the density of  $P_1$  for different values of precision ( $\tau$ ), with  $n = 10^3$ . If  $\tau = 1$ , the two models are equally right, and  $f(P_1) \rightarrow 1$  when  $n \rightarrow \infty$  so that  $P_1$  behaves like a  $\mathbb{U}(0, 1)$  random

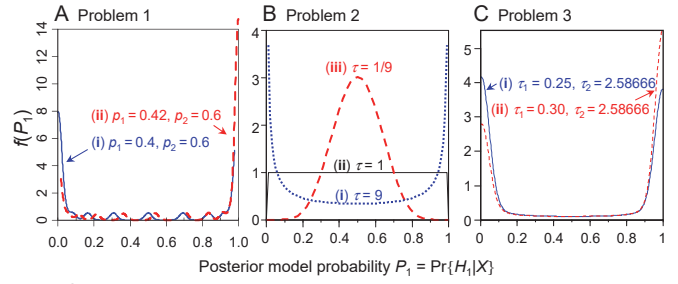


**Fig. 3.** The distribution of posterior model probability  $P_1 = \mathbb{P}\{H_1|x\}$  in three inference problems. (A) Problem 1 (fair-coin paradox) is for a coin-tossing experiment, where the true model is  $p = 0.5$  (a fair coin), and the compared models are (i)  $H_1 : p = 0.4$  and  $H_2 : p = 0.6$  so that the two models are equally wrong; and (ii)  $H_1 : p = 0.42$  and  $H_2 : p = 0.6$  so that  $H_1$  is less wrong than  $H_2$ . The data size (the number of coin tosses) is  $10^3$ . (B) Problem 2 (fair-balance paradox) is for a normal-distribution example in which the true model is  $\mathbb{N}(0, 1)$ , and the two compared models are  $H_1 : \mathbb{N}(\mu, 1/\tau)$ ,  $\mu < 0$  and  $H_2 : \mathbb{N}(\mu, 1/\tau)$ ,  $\mu > 0$ , with variance  $1/\tau$  given. The two models are equally right when  $\tau = 1$  and equally wrong but indistinct when  $\tau = 1/9$  or  $9$ . The data size is  $n = 10^3$ . The plots for  $n = 100$  or  $\infty$  are nearly the same. (C) Problem 3 (fair-balance paradox) is for a normal-distribution example in which the true model is  $\mathbb{N}(0, 1)$ , and the two compared models are  $H_1 : \mathbb{N}(\mu, 1/\tau_1)$  and  $H_2 : \mathbb{N}(\mu, 1/\tau_2)$ , with (i)  $\tau_1 = 0.25$  and  $\tau_2 = 2.58666$ , so that the two models are equally wrong and (ii)  $\tau_1 = 0.3$  and  $\tau_2 = 2.58666$ , so that  $H_1$  is less wrong than  $H_2$ . The prior is  $\mu \sim \mathbb{N}(0, 1/\xi)$  under each model, with  $\xi = 1$ . The data size is  $n = 100$ . All densities are estimated by simulating  $10^5$  samples for  $P_1$ .

number [11, 12]. If  $\tau < 1$ , the assumed variance ( $1/\tau$ ) is larger than the true variance, so that the distribution has a mode at  $\frac{1}{2}$ . If  $\tau > 1$ , the assumed variance is too small, and  $P_1$  has a U-shaped distribution. If one overstates the precision of the experiment, one tends to over-interpret the data and generate extreme posterior model probabilities. In all three cases ( $\tau < 1, = 1, > 1$ ),  $P_1$  has a non-degenerate distribution.

**Problem 3. Fair-balance paradox (equally wrong and distinct models).** The true model is  $\mathbb{N}(0, 1)$ , and the two compared models are  $H_1 : \mathbb{N}(\mu, 1/\tau_1)$  and  $H_2 : \mathbb{N}(\mu, 1/\tau_2)$ , with  $\tau_1 < 1 < \tau_2$  given, while  $\mu$  is a free parameter in each model. The best-fitting parameter value is  $\mu^* = 0$  in each model, irrespective of the value of  $\tau$  assumed. Both models are wrong because of the misspecified variance:  $H_1$  is over-dispersed while  $H_2$  is under-dispersed. They are equally wrong, in the sense that  $D_1 = D_2$  in eq. [1], if

$$\log \frac{\tau_1}{\tau_2} = \tau_1 - \tau_2 \quad [5]$$

(SI Appendix). This is a type-3 problem (Fig. 2,  $C_2$ ). We assign a uniform prior over the models ( $\frac{1}{2}$  each), and  $\mu \sim \mathbb{N}(0, 1/\xi)$ , with  $\xi$  given, within each model. The dataset, an i.i.d. sample of size  $n$  from  $\mathbb{N}(0, 1)$ , can be summarized as the sample mean  $\bar{x}$  and sample variance  $s^2 = \frac{1}{n} \sum_i (x_i - \bar{x})^2$ . The posterior odds is given in eq. (15) in SI Appendix.

We use  $\tau_1 = 0.25$  and  $\tau_2 = 2.58666$ , so that eq. [5] holds and the two models are equally wrong, to generate independent variables  $\bar{x} \sim \mathbb{N}(0, 1/n)$  and  $ns^2 \sim \chi_{n-2}^2$ , and to calculate  $P_1$ . Fig. 3C(i) shows the estimated density of  $P_1$  for  $n = 100$ , with  $\xi = 1$ . When  $n \rightarrow \infty$ ,  $P_1$  degenerates into a 2-point distribution at 0 and 1, each with probability  $\frac{1}{2}$ . This is the same dynamics as in Problem 1 (Fig. 3A(i)), even though in Problem 1 the models do not involve any unknown parameters while here they do.

Fig. 3C(ii) shows the density of  $P_1$  when  $\tau_1 = 0.3$  (which is closer to the true  $\tau = 1$  than is 0.25), so that  $H_1$  is less wrong than  $H_2$  (with  $D_1 < D_2$ ). In this case when  $n \rightarrow \infty$ ,  $P_1 \rightarrow 1$ . However, in large but finite datasets,  $P_2$  for the more wrong model  $H_2$  can be large in too many datasets: for example, with  $n = 100$ ,  $\mathbb{P}\{P_2 > 0.99\} = 0.0504$ :

in 5.04% of datasets, the more wrong model  $H_2$  has posterior higher than 99%.

**Star-tree paradox and Bayesian phylogenetics.** In Bayesian phylogenetics [1, 2], each model has two components: the phylogenetic tree describing the relationships among the species and the evolutionary model describing sequence evolution along the branches on the tree [19]. Each tree  $T_k$  has a set of time or branch length parameters ( $t_k$ ), which measure the amount of evolutionary changes along the branches. The evolutionary model may also involve unknown parameters ( $\psi$ ). The tree and the evolutionary model together specify the likelihood [20], with  $\theta = \{t, \psi\}$  to be the unknown parameters. One of the trees is true, and all other trees are wrong, while the evolutionary model may be misspecified. The main objective is to infer the true tree. The data consist of an alignment of sequences from the modern species, and have a multinomial distribution in which the categories correspond to the possible site patterns (configurations of nucleotides observed in the modern species) while the data size is the number of sites or alignment columns [21].

Here we consider three simple cases involving 3 or 4 species (Fig. 1). We use the general theory described above to predict the asymptotic behavior of posterior probabilities for trees and use computer simulation to verify the predictions.

Case A (Fig. 4A & A') involves equally right models. We use the rooted star tree  $T_0$  for three species with  $t = 0.2$  (Fig. 1A) to generate datasets to compare the three binary trees. The JC substitution model [22] is used both to generate and to analyze the data, which assumes that the rate of change between any two nucleotides is the same. The molecular clock (rate constancy over time) is assumed as well, so that the parameters in each binary tree are the two ages of nodes ( $t_0, t_1$ ), measured by the expected number of nucleotide changes per site.

The best-fitting parameter values are  $t_0^* = 0$  and  $t_1^* = 0.2$  for each of the three binary trees, in which case each binary tree converges to the true star tree. We assign uniform prior probabilities for the binary trees ( $\frac{1}{3}$  each), and exponential prior on branch lengths on each tree. According to our characterization, this is a type-2 problem of comparing equally right models (Fig. 2,  $B_2$ ), so the posterior probabilities should have a nondegenerate distribution. This case was considered in previous studies [12, 14, 15], which generated numerically the limiting distribution of the posterior probabilities for the binary trees ( $P_1, P_2, P_3$ ) when  $n \rightarrow \infty$ , and pointed out that they do not converge to  $(\frac{1}{3}, \frac{1}{3}, \frac{1}{3})$  [11, 12, 13].

Case B (Fig. 4B & B') involves equally wrong models that are indistinct. This is similar to case A except that the JC+ $\Gamma$  model [22, 23] is used to generate data, with different sites in the sequence evolving at variable rates according to the gamma distribution with shape parameter  $\alpha = 1$ . The data are then analyzed using JC (equivalently to JC+ $\Gamma$  with  $\alpha = \infty$ ). The best-fitting parameter values (i.e., the MLEs of branch lengths in infinite data) are  $t_0^* = 0$  and  $t_1^* = 0.16441$  under each of the three binary trees. The binary trees thus represent equally wrong models (with  $D_1 = D_2 = D_3 > 0$  in eq. [1]) that are indistinct. The posterior tree probabilities have a non-degenerate distribution. This is the type-2 'volatile' behavior for equal wrong and indistinct models (Fig. 2,  $B_4$ ).

Case C (Fig. 4C & C') involves equally wrong and distinct models. Like case B, the simulation model is JC+ $\Gamma$  with  $\alpha = 1$ , and the analysis model is JC. However, we do not assume the molecular clock and consider unrooted trees for four species (Fig. 1B). The true tree is the unrooted star tree  $T_0$  of Fig. 1B, with  $t_1 = t_2 = t_3 = t_4 = 0.2$ . The best-fitting parameter values (the MLEs of branch lengths in infinite data) are  $t_0^* = 0.01037, t_i^* = 0.16409, i = 1, 2, 3, 4$ , for each of the three binary trees (Fig. 1B). As  $t_0^* > 0$ , the three binary trees are different from the star tree and represent equally wrong and distinct models (with  $D_1 = D_2 = D_3 > 0$  in eq. [1]). As this is a type-3 problem (Fig. 2,  $C_4$ ), our theory predicts that as  $n \rightarrow \infty$ , the posterior probabilities for the three binary trees should degenerate into a three-

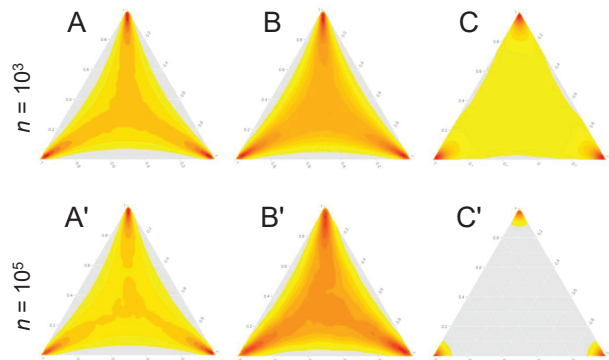


**Fig. 4.** The distribution of posterior probabilities ( $P_1, P_2, P_3$ ) for the three binary trees  $T_1, T_2$ , and  $T_3$  of Fig. 1, when datasets (sequence alignments of  $n = 10^3$  or  $10^5$  sites) are simulated using the star tree  $T_0$  and analyzed to compare the three binary trees. In (A) and (A'), the true tree is the star tree  $T_0$  for three species of Fig. 1A, with  $t = 0.2$ . Both the simulation and analysis models are JC, and the three binary trees are equally right models. In (B) and (B'), the true tree is the star tree  $T_0$  for three species of Fig. 1A, with  $t = 0.2$ . The simulation model is JC+ $\Gamma$  (with  $\alpha = 1$ ), and the analysis model is JC. The three binary trees represent equally wrong and indistinct models. In (C) and (C'), the true tree is the star tree  $T_0$  for four species of Fig. 1B, with  $t_1 = t_2 = t_3 = t_4 = 0.2$ . The simulation model is JC+ $\Gamma$  ( $\alpha = 1$ ) and the analysis model is JC. The three binary trees represent equally wrong and distinct models. The three corners in the plots correspond to points  $(1, 0, 0)$ ,  $(0, 1, 0)$ , and  $(0, 0, 1)$ , while the center is  $(\frac{1}{3}, \frac{1}{3}, \frac{1}{3})$ .

point distribution, with probability  $\frac{1}{3}$  each, for  $(1, 0, 0)$ ,  $(0, 1, 0)$ , and  $(0, 0, 1)$ . In other words, one of the binary trees will have posterior  $\sim 100\%$  while the other two will have  $\sim 0$ . This is confirmed by simulation (table 1).

We note that most phylogenetic analyses involve unrooted trees as the clock assumption is violated except for closely related species. Furthermore, because of the violation of the evolutionary model, all trees (or the joint tree-process models) represent wrong statistical models. Thus among the three cases considered in Fig. 4, case C is the most relevant to analysis of real data, when Bayesian model selection exhibits type-3 'polarized' behavior. Previous analyses of the star-tree paradox [12, 14, 15] have deplored the 'volatile' behavior of Bayesian phylogenetic method, but those studies examined case A only, so the real situation is worse than previously realized.

A practically important scenario is where all binary trees are wrong because of violation of the evolutionary model but the true tree is less wrong than the other trees. We present such a case in table 2, in which the data are simulated under JC+ $\Gamma$  (with  $\alpha = 1$ ) using a binary tree with a short internal branch ( $t_0 = 0.002$ ) and then analyzed under JC. When the amount of data approaches infinity, the true tree will eventually win, but there exists a twilight zone in which high posterior probabilities for wrong trees occur too frequently; according to table 2, this zone is wider than  $10^3 < n < 10^5$ . For example, at sequence length  $n = 10^4$  and at the 1% nominal level, the error rate of rejecting the true tree is 25.0% and the error rate of accepting a wrong tree is 16.6% (table 2).

## Discussion

**High posterior probabilities for phylogenetic trees.** This work has been motivated by the phylogeny problem, and in particular by the empirical observation of spuriously high posterior probabilities for phylogenetic trees [10, 11, 12, 13, 14, 9]. We note that certain biological processes such as deep coalescence [24, 25], gene duplication followed by gene loss [26], and horizontal gene transfer [26, 24] may cause different genes or genomic regions to have different histories. However, as discussed in Introduction, posterior probabilities

for many trees or clades observed in real data analyses are decidedly spurious even if the true tree is unknown.

One explanation for the spuriously high posterior probabilities for phylogenetic trees is the failure of current evolutionary models to accommodate interdependence among sites in the sequence, leading to an exaggeration of the amount of information in the data. Interacting sites may carry much less information than independent sites. This explanation predicts the problem to be more serious in coding genes than in noncoding regions of the genome as noncoding sites may be evolving largely independently due to lack of functional constraints. However, empirical evidence points to the opposite, with noncoding regions having higher substitution rates and higher information content (if they are not saturated with substitutions), generating more extreme posteriors for trees.

Our results suggest that the problem may lie deeper and may be a consequence of the polarized nature of Bayesian model selection. As the assumptions about the process of sequence evolution are unrealistic, the likelihood model is wrong whatever the tree, although the true tree may be expected to be less wrong than the other trees. As the different trees constitute opposing models that are nearly equally wrong, the inference problem is one of type-3 (Fig. 2,  $C_4$ ). Bayesian tree estimation may then be expected to produce extreme posterior probabilities in large datasets.

**Bayesian selection of opposing misspecified models.** We have provided a characterization of model selection problems according to the asymptotic behavior of the Bayesian method as the data size  $n \rightarrow \infty$  (Fig. 2 and SI Appendix). While all the problems considered here involve comparison of two ‘equally right’ or ‘equally wrong’ models, three different asymptotic behaviors are identified, which we label as type-1, type-2, and type-3. The type-1 behavior is for the posterior model probability  $P_1$  to converge to a sensible point value, such as  $\frac{1}{2}$ . We consider this to be a good ‘balanced’ behavior, following phylogeneticists [10, 11, 12]. The rationale is that one would like a sure answer given an infinite amount of data and the only reasonable sure answer should be  $\frac{1}{2}$  for each model, since the data contain no information for or against either model. This behavior occurs only when the two models are identical or overlapping, a situation that does not appear relevant to scientific inference. With type-2 behavior,  $P_1$  fluctuates among datasets (each of infinite size) like a random number, so that strong support may be attached to a particular model in some datasets. Biologists were surprised at this erratic behavior [10, 11, 12], which we label as ‘volatile’. This occurs when the models are equally right or equally wrong but indistinct. In theory, type-2 behavior may not pose a serious problem, because the parameter posteriors under the models, if examined carefully, should make it clear that the competing models essentially gave the same interpretation of the data and should lead to the same scientific conclusion. In data simulated in [12] or in Fig. 4A & A’, the estimates of  $t_0$  should be very close to 0, and all binary trees are similar to the same star tree. Nevertheless this escaped our attention at the time.

With type-3 behavior,  $P_1$  is  $\sim 0$  in half of the datasets, and  $\sim 1$  in the other half. We describe this behavior as ‘polarized’. This occurs when the two models are equally wrong and distinct. Type-3 problems may be the most relevant to practical data analysis given that all models are simplified representations of reality and are thus wrong. A variation to type-3 problems is when one model is only slightly less wrong than another (Figs. 3A(ii), 3C(ii), table 2). While the less wrong model eventually wins in the limit of infinite data, Bayesian model selection is over-confident in large but finite datasets, supporting the more wrong model with high posterior too often.

Note that the question of how the posterior model probability should behave when large datasets are used to compare two equally wrong models is somewhat philosophical and may not have a simple answer. One position is to accept whatever behavior the Bayesian method exhibits. This may be legitimate given that Bayesian the-

ory is the correct probability framework for summarizing evidence in the prior and likelihood. The polarized behavior in type-3 problems may then be seen as a consequence of ‘user error’ (for not including the true model in the comparison), exacerbated by the large data size. In this regard we note that the posterior predictive distribution [27, 28] can be used to assess the general adequacy of any model or the compatibility between the prior and the likelihood, and indeed this has been widely used to assess the goodness of fit of models in phylogenetics [29, 30]. Nevertheless, a number of sophisticated and parameter-rich models have been developed for Bayesian phylogenetic analysis, thanks to three decades of active research [31], and furthermore extreme sensitivity to the assumed model is not a desirable property of an inference method. Seven decades ago, Egon S. Pearson [32] wrote that “Hitherto the user has been accustomed to accept the function of probability theory laid down by the mathematicians; but it would be good if he could take a larger share in formulating himself what are the practical requirements that the theory should satisfy in application.” This stipulation may be relevant even today.

Two heuristic approaches have been suggested to remedy the high posterior model probabilities in the context of phylogenies. The first is to assign nonzero probabilities to multifurcating trees (such as the star tree of Fig. 1) in the prior [11]. This is equivalent to assigning some prior probability to the model  $p = 0.5$  in the fair-coin example of Problem 1. While this resolves the star-tree paradox, it suffers from the conceptual difficulty that the multifurcating trees may not be biologically . The second approach is to let the internal branch lengths in the binary trees become increasingly smaller in the prior when the data size increases [12, 14]. This is non-Bayesian in that the prior depends on the size of the data. With both approaches, the posterior is extremely sensitive to the prior [9].

**Non-Bayesian methods.** The phylogeny problem was described by Jerzy Neyman [33] as “a source of novel statistical problems”. In the Frequentist framework, test of phylogeny, or test of nonnested models in general, offers challenging inference problems. Note that in many model selection problems, the model itself is not the focus of interest. For example, when an experiment is conducted to evaluate the effect of a new fertilizer, the sensitivity of the inference to the assumed normal distribution with homogeneous variance may be of concern, but the focus is not on the normal distribution itself. In phylogenetics, the phylogeny (which is a model) is of primary interest, far more important than the branch lengths (which are parameters in the model). Test of phylogeny is thus more akin to significance/hypothesis testing than to model selection. Model-selection criteria such as AIC [34] or BIC [35] simply rank the trees by their likelihood (maximized over branch lengths), and will not be useful for attaching a measure of significance or confidence in the estimated tree. The phylogeny problem (or the problem of comparing nonnested models in general) falls outside the Fisher-Neyman-Pearson framework of hypothesis testing, which involves two nested models, one of which is true [36, 37].

In principle Cox’s likelihood ratio test [38], which conducts multiple tests with each model used as the null, can be used to compare nonnested models. For type-3 problems (Fig. 2,  $C_1$ - $C_4$ ), this test should lead to rejection of all models. Cox’s test has not been used widely in phylogenetics, apparently because of the existence of a great many possible trees and the heavy computation needed to generate the null distribution by simulation.

The most commonly used method for attaching a measure of confidence in the maximum likelihood tree is the bootstrap [39], which samples sites (alignment columns) to generate bootstrap pseudo-datasets and calculates the bootstrap support value for a clade (a node on the species tree) as the proportion of the pseudo-datasets in which that node is found in the inferred ML tree. This application of bootstrap for model comparison appears to have important differences from the conventional bootstrap for calculating the standard errors and confidence intervals for a parameter estimate [40]: a straightforward interpretation of the bootstrap support values for trees remains

elusive [41, 42, 43, 31]. At any rate, the asymptotic behavior of bootstrap support values under the different scenarios of Fig. 2 merits further research. For the fair-coin example of problem 1 (Fig. 2,  $C_1$ ), the bootstrap exhibits similar polarized behavior, although other cases are yet to be explored.

## Materials and Methods

Star-tree simulations. For Fig. 4A, A', B & B', the true tree is  $T_0$  of Fig. 1A. The data of counts of five site patterns ( $xxx$ ,  $xyx$ ,  $yxx$ ,  $xyx$ , and  $xyz$ ) were simulated by multinomial sampling [21], and analyzed using a C program, which calculates the

2-D integrals in the marginal likelihood by Gaussian-Legendre quadrature with 128 points [14]. For Fig. 4C & C', the true tree is  $T_0$  of Fig. 1B. Sequence alignments were simulated using EVOLVER and analyzed using MrBayes [4].

**ACKNOWLEDGMENTS.** We thank Philip Dawid and Wally Gilks for stimulating discussions, and Jeff Thorne and an anonymous reviewer for constructive comments. Z.Y. was supported by a Biotechnological and Biological Sciences Research Council grant (BB/P006493/1), and in part by the Radcliffe Institute for Advanced Study at Harvard University. T.Z. was supported by Natural Science Foundation of China grants (31671370, 31301093, 11201224 and 11301294) and a grant from the Youth Innovation Promotion Association of Chinese Academy of Sciences (2015080).

1. Rannala B, Yang Z (1996) Probability distribution of molecular evolutionary trees: a new method of phylogenetic inference. *J. Mol. Evol.* 43:304–311.
2. Mau B, Newton M (1997) Phylogenetic inference for binary data on dendrograms using markov chain monte carlo. *J. Computat. Graph. Stat.* 6:122–131.
3. Li S, Pearl D, Doss H (2000) Phylogenetic tree reconstruction using markov chain monte carlo. *J. Amer. Statist. Assoc.* 95:493–508.
4. Ronquist F, et al. (2012) MrBayes 3.2: Efficient Bayesian phylogenetic inference and model choice across a large model space. *Syst. Biol.* 61:539–542.
5. Bouckaert R, et al. (2014) Beast 2: a software platform for Bayesian evolutionary analysis. *PLoS Comput. Biol.* 10(4):e1003537.
6. Lartillot N, Lepage T, Blanquart S (2009) PhyloBayes 3: a Bayesian software package for phylogenetic reconstruction and molecular dating. *Bioinformatics* 25(17):2286–8.
7. Chen MH, Kuo L, Lewis P (2014) Bayesian Phylogenetics: Methods, Algorithms, and Applications. (Chapman and Hall/CRC).
8. Bourlat SJ, et al. (2006) Deuterostome phylogeny reveals monophyletic chordates and the new phylum xenoturbellida. *Nature* 444:85–88.
9. Yang Z (2008) Empirical evaluation of a prior for Bayesian phylogenetic inference. *Phil. Trans. R. Soc. Lond. B.* 363:4031–4039.
10. Suzuki Y, Glazko G, Nei M (2002) Overcredibility of molecular phylogenies obtained by Bayesian phylogenetics. *Proc. Natl. Acad. Sci. U.S.A.* 99:16138–16143.
11. Lewis P, Holder M, Holsinger K (2005) Polytomies and Bayesian phylogenetic inference. *Syst. Biol.* 54:241–253.
12. Yang Z, Rannala B (2005) Branch-length prior influences Bayesian posterior probability of phylogeny. *Syst. Biol.* 54:455–470.
13. Steel MA, Matsen F (2007) The Bayesian "star paradox" persists for long finite sequences. *Mol. Biol. Evol.* 24:1075–1079.
14. Yang Z (2007) Fair-balance paradox, star-tree paradox and Bayesian phylogenetics. *Mol. Biol. Evol.* 24:1639–1655.
15. Susko E (2008) On the distributions of bootstrap support and posterior distributions for a star tree. *Syst. Biol.* 57:602–612.
16. Dawid A (2011) Posterior model probabilities in Philosophy of Statistics, eds. Bandyopadhyay PS, Forster M. (Elsevier, New York), pp. 607–630.
17. Berk R (1966) Limiting behavior of posterior distributions when the model is incorrect. *Ann. Math. Statist.* 37:51–58.
18. White H (1982) Maximum likelihood estimation of misspecified models. *Econometrica* 50:1–25.
19. Yang Z, Goldman N, Friday AE (1995) Maximum likelihood trees from DNA sequences: a peculiar statistical estimation problem. *Syst. Biol.* 44:384–399.
20. Felsenstein J (1981) Evolutionary trees from DNA sequences: a maximum likelihood approach. *J. Mol. Evol.* 17:368–376.
21. Yang Z (1994) Statistical properties of the maximum likelihood method of phylogenetic estimation and comparison with distance matrix methods. *Syst. Biol.* 43:329–342.
22. Jukes T, Cantor C (1969) Evolution of protein molecules in *Molecular Protein Metabolism*, ed. Munro H. (Academic Press, New York), pp. 21–123.
23. Yang Z (1993) Maximum-likelihood estimation of phylogeny from DNA sequences when substitution rates differ over sites. *Mol. Biol. Evol.* 10:1396–1401.
24. Maddison W (1997) Gene trees in species trees. *Syst. Biol.* 46:523–536.
25. Xu B, Yang Z (2016) Challenges in species tree estimation under the multispecies coalescent model. *Genetics* 204:1353–1368.
26. Nichols R (2001) Gene trees and species trees are not the same. *Trends Ecol. Evol.* 16:358–364.
27. Roberts H (1965) Probabilistic prediction. *J. Am. Stat. Assoc.* 60:50–62.
28. Box G (1980) Sampling and Bayes' inference in scientific modelling and robustness. *J. R. Stat. Soc. A.* 143:383–430.
29. Sullivan J, Joyce P (2005) Model selection in phylogenetics. *Ann. Rev. Ecol. Evol. Syst.* 36:445–466.
30. Rodrigue N, Philippe H, Lartillot N (2006) Assessing site-interdependent phylogenetic models of sequence evolution. *Mol. Biol. Evol.* 23:1762–1775.
31. Yang Z (2014) *Molecular Evolution: A Statistical Approach*. (Oxford University Press, Oxford, England).
32. Pearson E (1947) The choice of statistical tests illustrated on the interpretation of data classed in the 2x2 table. *Biometrika* 34:139–167.
33. Neyman J (1971) Molecular studies of evolution: a source of novel statistical problems in Statistical decision theory and related topics, eds. Gupta SS, Yackel J. (Academic Press, New York), pp. 1–27.

34. Akaike H (1973) Information theory and an extension of the likelihood principle in *Proceedings of the Second International Symposium of Information Theory*, eds. Petrov BN, Csaki F. (Akademiai Kiado, Budapest), pp. 267–281.
35. Schwarz G (1978) Estimating the dimension of a model. *Ann. Statist.* 6:461–464.
36. Lehmann E (1997) *Testing statistical hypothesis*. (Springer-Verlag, New York), 2nd edition.
37. Goldman N, Anderson J, Rodrigo A (2000) Likelihood-based tests of topologies in phylogenetics. *Syst. Biol.* 49:652–670.
38. Cox D (1961) Tests of separate families of hypotheses. *Proc. 4th Berkeley Symp. Math. Stat. Prob.* 1:105–123.
39. Felsenstein J (1985) Confidence limits on phylogenies: an approach using the bootstrap. *Evolution* 39:783–791.
40. Efron B, Tibshirani R (1993) *An Introduction to the Bootstrap*. (Chapman and Hall, London).
41. Felsenstein J, Kishino H (1993) Is there something wrong with the bootstrap on phylogenies? a reply to hillis and bull. *Syst. Biol.* 42:193–200.
42. Efron B, Halloran E, Holmes S (1996) Bootstrap confidence levels for phylogenetic trees [corrected and republished article originally printed in *proc. natl. acad. sci. u.s.a.* 1996. 93:7085–7090]. *Proc. Natl. Acad. Sci. U.S.A.* 93:13429–13434.
43. Susko E (2009) Bootstrap support is not first-order correct. *Syst. Biol.* 58(2):211–223.

**Table 1. Proportions of datasets with extreme posterior probabilities for the three binary trees in the star-tree simulation.  $P_{\max} = \max(P_1, P_2, P_3)$  and  $P_{\min} = \min(P_1, P_2, P_3)$ . Data are generated under  $JC+\Gamma$  with  $\alpha = 1$  using the star tree for four species: ( $a : 0.2, b : 0.2, c : 0.2, d : 0.2$ ), and analyzed under  $JC$ . The number of replicates is  $10^3$ . The probability density of  $(P_1, P_2, P_3)$  for the case of  $N = 10^3$  and  $10^5$  are shown in Fig. 4C and 4C'.**

$n$	$\mathbb{P}\{P_{\min} < 1\%\}$	$\mathbb{P}\{P_{\min} < 5\%\}$	$\mathbb{P}\{P_{\max} > 95\%\}$	$\mathbb{P}\{P_{\max} > 99\%\}$	$E(P_{\min})$	$E(P_{\max})$
$10^3$	0.234	0.550	0.205	0.079	0.067	0.754
$10^4$	0.812	0.931	0.606	0.450	0.011	0.897
$10^5$	0.979	0.992	0.853	0.773	0.001	0.964
$10^6$	1.000	1.000	0.953	0.919	0.000	0.988
$10^7$	1.000	1.000	0.982	0.970	0.000	0.995

**Table 2. Proportions of datasets with strong support for wrong trees in simulated datasets for four species.  $P_{23} = \max(P_2, P_3)$ . Data are generated under  $JC+\Gamma$  (with  $\alpha = 1$ ) and analyzed under  $JC$ . The true tree is  $T_1$  of Fig. 1B: ( $a : 0.2, b : 0.2$ ) : 0.002,  $c : 0.2, d : 0.2$ , so that  $T_2$  and  $T_3$  are the two wrong trees in the analysis. The number of replicates is  $10^3$ .**

$n$	$\mathbb{P}\{P_1 < 1\%\}$	$\mathbb{P}\{P_1 < 5\%\}$	$\mathbb{P}\{P_{23} > 0.95\%\}$	$\mathbb{P}\{P_{23} > 99\%\}$
$10^3$	0.083	0.225	0.113	0.038
$10^4$	0.250	0.337	0.266	0.166
$10^5$	0.102	0.120	0.115	0.097
$10^6$	0.000	0.000	0.000	0.000
$10^7$	0.000	0.000	0.000	0.000

## Supplemental Information Appendix

**General theory for equally wrong models with no free parameters ( $d = 0$ ).** The data,  $x = \{x_i\}$ , consist of an i.i.d. sample from the true model  $g(\cdot)$ ; that is,  $x_i \sim g(x_i)$ ,  $i = 1, 2, \dots, n$ . We consider two models  $H_1$  and  $H_2$ , with densities  $f_1(x)$  and  $f_2(x)$ , respectively. The models are equally wrong, with  $D_1 = D_2 > 0$  in eq. [1] in the main text, and also identifiable. We assign a uniform prior ( $\pi_k = \frac{1}{2}$  each) on the two models. With no parameters in either model, the marginal likelihood ( $M$ ) is the same as the likelihood ( $L$ ), so that the logarithm of the marginal likelihood ratio is

$$\Delta_n = \log \frac{M_1}{M_2} = \log \frac{L_1}{L_2} = \sum_i^n \log \frac{f_1(x_i)}{f_2(x_i)} = \sum_i^n r_i. \quad (1)$$

Thus  $\Delta_n$  is a sum of  $n$  i.i.d. random variables ( $r_i$ ).

For large  $n$ ,  $\Delta_n$  has approximately a normal distribution by the central-limit theorem, with mean

$$\mathbb{E}_g(\Delta_n) = \mathbb{E}_g \left\{ \sum_i^n r_i \right\} = n \int g(x) \log \frac{f_1(x)}{f_2(x)} dx = n(D_1 - D_2) = 0 \quad (2)$$

and variance

$$\mathbb{V}_g(\Delta_n) = \mathbb{E}_g \left\{ \sum_i^n r_i^2 \right\} = n \int g(x) \left[ \log \frac{f_1(x)}{f_2(x)} \right]^2 dx = nC, \quad (3)$$

with  $C > 0$ , since the two models are distinct. Note that  $P_1 = \frac{1}{1+1/e^{\Delta_n}}$ . For  $P_1$  to be not extreme,  $\Delta_n$  should be close to 0.  $P_1$  is in the interval  $(\alpha, 1 - \alpha)$  for small  $\alpha$ , if and only if  $|\Delta_n| < A = \log \frac{1-\alpha}{\alpha}$ . With large  $n$ , this occurs with probability

$$\mathbb{P}\{|\Delta_n| < A\} \approx 1 - 2\Phi\left(-\frac{A}{\sqrt{nC}}\right) \approx \frac{2A}{\sqrt{2\pi nC}}. \quad (4)$$

In Problem 1 (fair coin paradox),  $r_i$  has a two-point distribution taking values  $\pm \log \frac{0.4}{0.6}$ , each with probability  $\frac{1}{2}$ , so that  $\Delta_n$  ( $n = 0, 1, \dots$ ) constitutes a discrete-step random walk. We have  $\mathbb{E}_g(\Delta_n) = 0$  and  $\mathbb{V}_g(\Delta_n) = nC = n \left[ \log \frac{0.4}{0.6} \right]^2$ , and eq. (4) agrees with eq. 3 in the main text.

We are interested in the Frequentist properties of Bayesian model selection. If we generate many replicate datasets under the true model  $g(x)$  and analyze each to calculate  $P_1$ , the proportion of datasets in which  $P_1$  lies in the interval  $(\alpha, 1 - \alpha)$  goes to 0 at the rate of  $n^{-\frac{1}{2}}$ . In the limit when  $n \rightarrow \infty$ ,  $P_1 \rightarrow 0$  in half of the datasets and  $\rightarrow 1$  in the other half. Previously Berk [1] discussed the case of two equally wrong models represented by  $\theta = 0$  and 1, noting that asymptotically the posterior model probability does not converge to a point value.

We say that  $\Delta_n$  is of order  $n^{\frac{1}{2}}$ , or  $\Delta_n = \Theta_p(n^{\frac{1}{2}})$ . Formally  $Y_n = \Theta_p(a_n)$  if for any given probability  $\varepsilon > 0$ , there exist  $N, A_1(N, \varepsilon) > 0$  and  $A_2(N, \varepsilon) > 0$ , such that when  $n > N$ , we have

$$\mathbb{P}\{A_1 < |Y_n/a_n| < A_2\} > 1 - \varepsilon. \quad (5)$$

Effectively  $Y_n$  increases with  $n$  no faster than  $a_n$  and no more slowly than  $a_n$ . Using eqs. (2) and (3), with  $Y_n = \Delta_n$  and  $a_n = \sqrt{n}$ , it is easy to confirm that eq. (5) is satisfied if  $A_1 = C^{\frac{1}{2}}\Phi^{-1}\left(\frac{1}{2} + \frac{\varepsilon}{4}\right)$  and  $A_2 = C^{\frac{1}{2}}\Phi^{-1}\left(1 - \frac{\varepsilon}{4}\right)$ . Thus when  $n$  increases,  $|\Delta_n|$  increases no faster than  $\sqrt{n}$  and no more slowly than  $\sqrt{n}$ .

The above argument applies to any pair of models in the case of comparing  $K$  equally wrong models. With probability  $1/K$  (i.e., in  $1/K$  of the datasets), the posterior model probability for one of the models  $\rightarrow 1$  while all others  $\rightarrow 0$ , when  $n \rightarrow \infty$ .

Note the assumption that the two models are equally wrong, with  $E_g(\Delta_n) = 0$  or  $D_1 = D_2 > 0$ . Otherwise if  $D_1 \neq D_2$ ,  $\Delta_n = n(D_1 - D_2)$  is  $\Theta_p(n)$  and the less wrong model will dominate.

**General theory for equally right or equally wrong models with free parameters ( $d > 0$ ).** The data ( $x$ ) are generated from the density  $g(\cdot)$ , and we compare two models  $H_1$  and  $H_2$ . Model  $H_1$  specifies the density  $f_1(x|\theta_1)$  with  $d_1$  parameters ( $\theta_1$ ), while  $H_2$  has density  $f_2(x|\theta_2)$  with  $d_2$  parameters ( $\theta_2$ ). For any dataset,  $x = \{x_1, \dots, x_n\}$ , the MLE  $\hat{\theta}_k$  maximizes the likelihood function  $f_k(x|\theta_k)$  under model  $H_k$ . When  $n \rightarrow \infty$ ,  $\hat{\theta}_k \rightarrow \theta_k^*$ . Thus  $\hat{\theta}_k$  may be considered a natural estimate of  $\theta_k^*$  [2]. As usual, we assume that both  $\hat{\theta}_k$  and  $\theta_k^*$  are inner points in the parameter space of  $H_k$ . Whether  $\theta_k^*$  is inside the parameter space or at its boundary should affect the precise distribution of  $P_1$  but not its dynamics (i.e., whether or not  $P_1$  has a degenerate distribution).

As in [2], we define two matrices:

$$\begin{aligned} I_k(\theta_k) &= \mathbb{E}_g \{ \nabla \log f_k(x|\theta_k) \cdot \nabla \log f_k(x|\theta_k)^T \}, \\ J_k(\theta_k) &= \mathbb{E}_g \{ -\nabla^2 \log f_k(x|\theta_k) \}, \end{aligned} \quad (6)$$

where the expectation is over the true distribution  $x \sim g(\cdot)$ , and where  $\nabla$  and  $\nabla^2$  are the first and second derivatives with respect to  $\theta_k$ .

Following [3], we decompose the marginal likelihood  $M_k = f_k(x)$ ,  $k = 1, 2$ , as a product of three terms, so that

$$\log \frac{M_k}{g(x)} = \log \frac{f_k(x)}{f_k(x|\hat{\theta}_k)} + \log \frac{f_k(x|\hat{\theta}_k)}{f_k(x|\theta_k^*)} + \log \frac{f_k(x|\theta_k^*)}{g(x)} := A_k + B_k + C_k. \quad (7)$$

We define the corresponding differences between the two models as  $\Delta A = A_1 - A_2$ ,  $\Delta B = B_1 - B_2$ , and  $\Delta C = C_1 - C_2$ , with

$$\Delta := \log \frac{M_1}{M_2} = \Delta A + \Delta B + \Delta C. \quad (8)$$

From eq. (6) of [3], the first term in eq. (8) is

$$\Delta A = -\frac{d_1 - d_2}{2} \log \frac{n}{2\pi} + \log \frac{f_1(\theta_1^*)}{f_2(\theta_2^*)} + \log \left( \frac{\det J_2^*}{\det J_1^*} \right)^{\frac{1}{2}} + \Theta_p(n^{-\frac{1}{2}}), \quad (9)$$

where  $J_k^* = J_k(\theta_k^*)$  is  $J_k(\theta_k)$  evaluated at  $\theta_k^*$ , and  $\det Z$  is the determinant of matrix  $Z$ .

For the second term in eq. (8),  $\Delta B$ , we have

$$B_k \approx \frac{1}{2} \{ \sqrt{n}(\hat{\theta}_k - \theta_k^*) \}^T J_k^* \{ \sqrt{n}(\hat{\theta}_k - \theta_k^*) \} \quad (10)$$

[3, eq. A.8]. As  $\sqrt{n}(\hat{\theta}_k - \theta_k^*)$  converges in distribution to  $\mathbb{N}(0, [(J_k^*)^{-1}]^T I_k^* (J_k^*)^{-1})$  [2, Theorem 3.2],  $B_k$  and thus  $\Delta B$  are  $\Theta_p(1)$ . Here  $I_k^* = I_k(\theta_k^*)$  is  $I_k(\theta_k)$  evaluated at  $\theta_k^*$ . In the special case that model  $H_k$  is correct,  $I_k^* = J_k^*$  and  $B_k$  converges to  $\frac{1}{2} \chi_{d_k}^2$  in distribution.  $\Delta B$  is then the difference of two (correlated)  $\frac{1}{2} \chi_{d_k}^2$  variables.

Finally, the third term in eq. (8),  $\Delta C = \log \frac{f_1(x|\theta_1^*)}{f_2(x|\theta_2^*)}$  is identically 0 if the two models are indistinct, that is, if  $f_1(x|\theta_1^*) = f_2(x|\theta_2^*)$  almost everywhere, as in the type-1 and type-2 problems of Fig. 2. Otherwise  $\Delta C$  is of  $\Theta_p(n^{\frac{1}{2}})$ , given by the random walk (eq. (1)). As in

## Reserved for Publication Footnotes

the case of no parameters discussed above, we assume that the two models are equally wrong, with  $D_1 = D_2$  or  $\mathbb{E}_g(\Delta C) = 0$ . Otherwise  $\Delta C$  is  $\Theta_p(n)$  and dominates  $\Delta A$  and  $\Delta B$ : the less wrong model will dominate with posterior probability approaching 1.

The order of the three terms in eq. (8) is summarized in table S1. First is the case where the two models are indistinct. We have  $\Delta C = 0$  and  $\Delta B = \Theta_p(1)$ , while  $\Delta A = \Theta_p(1)$  if  $d_1 = d_2$  and  $\Delta A = \Theta(\log(n))$  if  $d_1 \neq d_2$ . If the two models have the same dimension ( $d_1 = d_2$ ),  $\Delta$  is of order  $\Theta_p(1)$  and converges to a non-degenerate distribution, which is determined by both  $\Delta A$  and  $\Delta B$ . This is the type-2 behavior of Fig. 2. If  $d_1 \neq d_2$ , the  $\log n$  term in eq. (9) dominates, so that the model with fewer parameters wins. It is noteworthy that as long as the two models are indistinct (and no matter whether they are equally right or equally wrong), the model with fewer parameters wins.

Next is the case where the two models are distinct. We have  $\Delta A$  is  $\Theta(1)$  if  $d_1 = d_2$  or  $\Theta(\log(n))$  if  $d_1 \neq d_2$ ,  $\Delta B$  is  $\Theta_p(1)$  and  $\Delta C$  is  $\Theta_p(\sqrt{n})$ , so that  $\Delta C$  dominates. Whether or not the two models have the same dimension,  $\Delta$  behaves like a random walk with mean 0 and variance of order  $n$ . In this case,  $P_1 \rightarrow 1$  in half of the datasets and  $\rightarrow 0$  in the other half. The case with  $d_1 = d_2$  is illustrated as the type-3 behavior of Fig. 2. Note that when the two models are equally wrong and distinct, the size of the model does not matter and the model with fewer parameters does not dominate.

**Analysis of Problem 2 (two equally right models or equally wrong but indistinct models).** The true model is  $\mathbb{N}(0, 1)$ , and we compare two models  $H_1: \mathbb{N}(\mu, 1/\tau)$ ,  $\mu < 0$  and  $H_2: \mathbb{N}(\mu, 1/\tau)$ ,  $\mu > 0$ , with  $\tau$  given. The MLE in infinite data is  $\mu^* = 0$  in each model, and the two models are indistinct. The data ( $x$ ) are summarized as the sample mean  $\bar{x}$ . We assign uniform prior (with 1/2 each) for the two models, and  $\mu \sim \mathbb{N}(0, 1/\xi)$ , with  $\xi$  given, truncated to the appropriate range under each model. The posterior model probability  $P_1$  can be derived by considering the posterior of  $\mu$  under the model  $\mathbb{N}(\mu, 1/\tau)$  with  $-\infty < \mu < \infty$ . As the prior precision is  $\xi$  and the data (likelihood) precision is  $n\tau$ , the posterior of  $\mu$  is  $\mu|x \sim \mathbb{N}\left(\frac{n\tau\bar{x}}{n\tau+\xi}, \frac{1}{n\tau+\xi}\right)$ . Thus

$$P_1 = \mathbb{P}\{H_1|x\} = \mathbb{P}\{\mu < 0|x\} = \Phi\left(-\frac{n\tau\bar{x}}{\sqrt{n\tau+\xi}}\right). \quad (11)$$

As  $\bar{x}$  varies among datasets according to  $\mathbb{N}(0, 1/n)$ , we have  $P_1 \approx \Phi(z\sqrt{\tau})$  if  $n$  is large, where  $z = -\sqrt{n}\bar{x} \sim \mathbb{N}(0, 1)$ . The density of  $P_1$  is given by a variable transform. Note that  $\left|\frac{dP_1}{d\bar{x}}\right| = \phi\left(-\frac{n\tau\bar{x}}{\sqrt{n\tau+\xi}}\right) \times \frac{n\tau}{\sqrt{n\tau+\xi}}$ , where  $\phi(x)$  is the probability density function (PDF) for  $\mathbb{N}(0, 1)$ , and  $\bar{x} = -\Phi^{-1}(P_1)\frac{\sqrt{n\tau+\xi}}{n\tau}$ .

$$\begin{aligned} f(P_1) &= \phi(\bar{x}; 0, \frac{1}{n}) \left/ \left| \frac{dP_1}{d\bar{x}} \right| \right. \\ &= \frac{1}{\sqrt{2\pi/n}} e^{-\frac{1}{2}n\bar{x}^2} \times \sqrt{2\pi} \cdot e^{\frac{1}{2}\frac{(n\tau\bar{x})^2}{n\tau+\xi}} \times \frac{\sqrt{n\tau+\xi}}{n\tau} \\ &= \frac{\sqrt{\tau+\xi/n}}{\tau} \cdot \exp\left\{\frac{n}{2}\bar{x}^2 \left[\frac{n\tau^2}{n\tau+\xi} - 1\right]\right\} \\ &= \frac{\sqrt{\tau+\xi/n}}{\tau} \cdot \exp\left\{\frac{n}{2}[\Phi^{-1}(P_1)]^2 \cdot \frac{n\tau+\xi}{(n\tau)^2} \left[\frac{n\tau^2}{n\tau+\xi} - 1\right]\right\} \\ &= \frac{\sqrt{\tau+\xi/n}}{\tau} \cdot \exp\left\{\frac{1}{2}[\Phi^{-1}(P_1)]^2 \left[1 - \frac{1}{\tau} - \frac{\xi}{n\tau^2}\right]\right\}, \quad (12) \end{aligned}$$

where  $\phi(x; \mu, \sigma^2)$  is the PDF for  $x \sim \mathbb{N}(\mu, \sigma^2)$ . This is eq. 4 in the main text.

**Analysis of Problem 3 (two equally wrong and distinct models, Gaussian with incorrect variances).** Suppose the true model is  $\mathbb{N}(0, 1)$ , and two compared models are  $H_1: \mathbb{N}(\mu, 1/\tau_1)$  and  $H_2: \mathbb{N}(\mu, 1/\tau_2)$ , with  $\tau_1 < 1 < \tau_2$  given, while  $\mu$  is a free parameter. The K-L divergence from model  $H_1$  with parameter  $\mu$  to the true model is

$$D_1(\mu) = \int \phi(x) \log \frac{\phi(x)}{\phi(x; \mu, 1/\tau_1)} dx. \quad (13)$$

$D_1(\mu)$  is minimized at  $\mu^* = 0$ . Similarly for model  $H_2$ ,  $D_2(\mu)$  is minimized at  $\mu^* = 0$ . Letting  $D_1(\mu^*) = D_2(\mu^*)$  so that the two models are equally wrong leads to  $\log \frac{\tau_1}{\tau_2} = (\tau_1 - \tau_2)$ . In general, if the true model is  $\mathbb{N}(\mu, 1/\tau_0)$ , then  $H_1$  and  $H_2$  are equally wrong if  $\tau_0 = (\tau_1 - \tau_2) / \log \frac{\tau_1}{\tau_2}$ .

We assign a uniform prior (1/2 each) for the two models, and  $\mu \sim \mathbb{N}(0, 1/\xi)$  under each model, with  $\xi$  given. The data are summarized as the sample mean  $\bar{x}$  and sample variance  $s^2 = \frac{1}{n} \sum_i (x_i - \bar{x})^2$ . The marginal likelihood under  $H_1$  is

$$\begin{aligned} M_1 &= \int_{-\infty}^{\infty} \frac{1}{\sqrt{2\pi/\xi}} e^{-\frac{\xi}{2}\mu^2} \cdot \left(\frac{1}{\sqrt{2\pi/\tau_1}}\right)^n \exp\left\{-\frac{1}{2}\tau_1 \sum_i (x_i - \mu)^2\right\} d\mu \\ &= \sqrt{\frac{\xi}{2\pi}} \left(\frac{\tau_1}{2\pi}\right)^{\frac{n}{2}} \int_{-\infty}^{\infty} \exp\left\{-\frac{1}{2}(\xi + n\tau_1)\mu^2 + n\tau_1\bar{x}\mu - \frac{1}{2}\tau_1 \sum_i x_i^2\right\} d\mu \\ &= \sqrt{\frac{\xi}{2\pi}} \left(\frac{\tau_1}{2\pi}\right)^{\frac{n}{2}} \times \sqrt{\frac{2\pi}{\xi + n\tau_1}} \exp\left\{-\frac{1}{2}n\tau_1 \left(\bar{x}^2 + s^2 - \frac{n\tau_1\bar{x}^2}{\xi + n\tau_1}\right)\right\} \\ &= \sqrt{\frac{\xi}{\xi + n\tau_1}} \left(\frac{\tau_1}{2\pi}\right)^{\frac{n}{2}} \times \exp\left\{-\frac{n\tau_1}{2(\xi + n\tau_1)} [\xi\bar{x}^2 + \xi s^2 + n\tau_1 s^2]\right\}. \quad (14) \end{aligned}$$

With the marginal likelihood  $M_2$  under  $H_2$  similarly given, the posterior odds is

$$\begin{aligned} \frac{P_1}{P_2} &= \sqrt{\frac{\xi + n\tau_2}{\xi + n\tau_1}} \left[\frac{\tau_1}{\tau_2}\right]^{\frac{n}{2}} \exp\left\{\frac{n}{2(\xi + n\tau_1)(\xi + n\tau_2)}\right. \\ &\quad \left. \times [(\tau_2 - \tau_1)(\xi^2\bar{x}^2 + \xi^2 s^2 + n\tau_1\tau_2 s^2) + (\tau_2^2 - \tau_1^2)n\xi s^2]\right\}. \quad (15) \end{aligned}$$

The distribution of  $P_1$  is given as a transform of  $\bar{x}$  and  $s^2$ , but the derivation is tedious. Instead we generate a sample of  $P_1$  by simulating random variables  $\bar{x} \sim \mathbb{N}(0, 1/n)$  and  $ns^2 \sim \chi_{n-1}^2$ .

When  $n \rightarrow \infty$ , we obtain, using eq. 5 in the main text,

$$\frac{P_1}{P_2} = \frac{M_1}{M_2} \rightarrow e^{\frac{1}{2}(\tau_2 - \tau_1)(ns^2 - (n-1))} \rightarrow e^{\frac{1}{2}(\tau_2 - \tau_1)Z}, \quad (16)$$

where  $Z = ns^2 - (n-1) \sim \mathbb{N}(0, 2n-2)$  because for large  $n$ ,  $\chi_{n-1}^2$  is approximately  $\mathbb{N}(n-1, 2n-2)$ . Thus when  $n$  is large,  $Z$  will have a vanishingly small probability of lying in a fixed interval around 0, and  $P_1$  will be either  $\sim 0$  or  $\sim 1$ , each in half of the datasets.

**Star-tree simulation.** We consider three cases, involving trees of three or four species only.

In case 1 (Fig. 4A & A'), the molecular clock (rate constancy over time) is assumed, and the true tree is the star tree for three species of Fig. 1A, with the branch length  $t = 0.2$  (changes per site on average). The JC substitution model [4] is used both to generate and to analyze the data. The three binary trees ( $T_1, T_2, T_3$ ) represent three equally right models. We assign a uniform prior ( $\frac{1}{3}$  each) on the binary trees, and given each binary tree, exponential priors with means 0.1 for  $t_0$  and 0.2 for  $t_1$ . The marginal likelihoods or the 2-D integrals over  $t_0$  and  $t_1$  are calculated numerically using Gaussian quadrature [5].

Case 2 (Fig. 4B & B') is similar to case 1, except that the substitution model used in the simulation is JC+ $\Gamma$  [4, 6], with different sites in the sequence evolving at variable rates according to the gamma



distribution with shape parameter  $\alpha = 1$ . The analysis model is still JC (equivalently to JC+ $\Gamma$  with  $\alpha = \infty$ ). The MLE at the limit of infinite data is  $t_0^* = 0$  in each binary tree, so that the three models under comparison are equally wrong and indistinct.

In case 3 (Fig. 4C & C') the true model is JC+ $\Gamma$  with  $\alpha = 1$  and the analysis model is JC, as in case 2, but we simulate data using an unrooted star tree for four species. The true branch lengths are  $t_1 = t_2 = t_3 = t_4 = 0.2$  in  $T_0$  (Fig. 1B). The data are analyzed to evaluate the three binary unrooted trees for four species (Fig. 1B), each with five branch lengths, without assuming the molecular clock. Be-

cause the MLE  $t_0^* > 0$  in the binary trees in the limit of infinite data, this case is a comparison of equally wrong and distinct models. The three binary trees are assigned equal prior probabilities ( $\frac{1}{3}$  each), and the five branch lengths in each tree are assigned the exponential prior with mean 0.1. The program MrBayes [7] is used to calculate the posterior probabilities for the three binary trees ( $P_1, P_2, P_3$ ) by MCMC. The program is tricked into collapsing the  $n$  sites into 15 (instead of 256) site patterns to speed up the likelihood calculation. Each MCMC run, for  $2 \times 10^6$  iterations, takes  $\sim 10$  seconds.

1. Berk R (1966) Limiting behavior of posterior distributions when the model is incorrect. *Ann. Math. Statist.* 37:51–58.
2. White H (1982) Maximum likelihood estimation of misspecified models. *Econometrica* 50:1–25.
3. Dawid A (2011) Posterior model probabilities in *Philosophy of Statistics*, eds. Bandyopadhyay PS, Forster M. (Elsevier, New York), pp. 607–630.
4. Jukes T, Cantor C (1969) Evolution of protein molecules in *Mammalian Protein Metabolism*, ed. Munro H. (Academic Press, New York), pp. 21–123.
5. Yang Z (2007) Fair-balance paradox, star-tree paradox and Bayesian phylogenetics. *Mol. Biol. Evol.* 24:1639–1655.
6. Yang Z (1993) Maximum-likelihood estimation of phylogeny from DNA sequences when substitution rates differ over sites. *Mol. Biol. Evol.* 10:1396–1401.
7. Ronquist F, et al. (2012) Mrbayes 3.2: Efficient Bayesian phylogenetic inference and model choice across a large model space. *Syst. Biol.* 61:539–542.

**Table 1. Table S1. The order of the three terms ( $\Delta A, \Delta B$ , and  $\Delta C$ ) in eq. (8) and the asymptotic behavior of Bayesian model selection**

	$\Delta A$	$\Delta B$	$\Delta C$	Behavior of Bayesian model selection
Indistinct models				
$d_1 = d_2$	$\Theta_p(1)$	$\Theta_p(1)$	0	Converges to a nondegenerate distribution
$d_1 < d_2$	$\Theta(\log(n))$	$\Theta_p(1)$	0	Model with fewer parameters dominates
Distinct models				
$d_1 = d_2$	$\Theta_p(1)$	$\Theta_p(1)$	$\Theta_p(n^{\frac{1}{2}})$	Random walk
$d_1 \neq d_2$	$\Theta_p(\log n)$	$\Theta_p(1)$	$\Theta_p(n^{\frac{1}{2}})$	Random walk